International Journal of Advanced Research in Chemical Science (IJARCS)
Volume 1, Issue 2, April 2014, PP 28-37
ISSN 2349-039X (Print) & ISSN 2349-0403 (Online)
www.arcjournals.org

Synthesis and Characterisation of Ag and Nitrogen Doped Tio_2 Nanoparticles Supported on A Chitosan-Pvae Nanofibre Support

Atsile Rosy Ocwelwang, Lilian Tichagwa

Nanotechnology and Water Treatment Research Group, Department of Chemistry,
University of Fort Hare, Private Bag X1314, Alice 5700, South Africa
ltichagwa@gmail.com
Atsile.rosy@gmail.com

Abstract: *In this studythe sol gel synthesis method was employed for the preparation of nitrogen and silver-doped TiO_2nanoparticles.This was followed by immobilising the prepared nanoparticles onto chitosan (Cs) and polyvinyl alcohol-co-ethylene (PVAE) polymer fibres using the process of electrospinning. This was done so as to secure the particles on the Cs/PVAE matrix to allow their use in applications such as water treatment. Characterisation was carried out to establish some physical properties of the prepared particles. Transmission Electron Microscopy (TEM), Scanning Electron Microscopy (SEM) and Energy-dispersive x-ray Spectroscopy (EDX) were used to analyze the size, morphology and composition of the nanomaterials. Fourier Transform Infrared (FTIR) spectroscopy was used to monitor reactions and for identification of functional groups while X-ray diffraction (XRD) analysis was carried out to determine the crystalline phases of the synthesized material. The crystallite size was calculated using the Scherrer equation and the thermal stability of the nanocomposites was determined using Thermogravimetric analysis(TGA).The XRD patterns showed that the undoped and doped samples consisted of mixed crystalline phases of anatase and rutile. The diameter of randomly selected nanoparticles was found to range from 6.4 nm to 21 nm while the size of the nanofibres was found to be in the range 234-270 nm. Nitrogen doped titania nanoparticles were the smallest in size.*

Keywords: *Titanium dioxide, poly(vinyl alcohol-co-ethylene), Chitosan, nanoparticles, doping, electrospinning, sol gel*

1. INTRODUCTION

The world is facing adverse challenges in meeting the growing demand for potable water due to a variety of reasons which include climate change, water pollution and depletion of the few available fresh water resources due to population growth. Lack of potable water has led to various water borne diseases and developing countries are more susceptible(Arnel, 2004; Savage, 2009). Both developing and developed countries are continuously facing an increase in water contamination from a variety of sources including a variety of human activities (Shannon et al., 2008).

These problems have fuelled research on the synthesis and application of nanocomposite materials with good pollutant removal properties. Advanced oxidation technologies (AOTs) for water treatment withtitanium dioxide (TiO_2) photocatalysisis one of the promising methods for water treatment(Choi etal., 2007). Silver, Ag and Chitosan have been reported to possess disinfectant properties while TiO_2has been found to be effective in generating hydroxyl radicals that can degrade organic pollutants to carbon dioxide (CO_2) and water (H_2O). A composite of Chitosan and Ag with TiO_2 should be able to inactivate microorganic pathogens in water as well as degrade organic pollutants at the same time. TiO_2 is a good photocatalyst due to its relative biocompatibility, its high efficiency, relatively low production costs and chemical inertness(Nor et al., 2009).

Even though the use of TiO_2 promises better prospects in water treatment, one setback is separation of the TiO_2 powder from water after photocatalytic reactions for reuse and possible environmental contamination by the nanoparticlesafter they have been used (Nosaka et al., 2005; Kim et al., 2008).To overcome this predicament, immobilization of the photocatalyst on a polymeric support has often been proposed. Coupling of titania nanoparticles with electrospun polymer nanofibres has been reported to be a practical and an efficient approach that leads to improved photocatalytic properties of TiO_2(Su et al., 2003). This work reports on the sol-gel synthesis and characterization of TiO_2 nanoparticles doped with silver (Ag) and nitrogen (N)and subsequent immobilization on a substrate blend of chitosan (Cs)and poly (vinyl alcohol-co-ethylene) (PVAE) polymers using theelectrospining method.

2. EXPERIMENTAL

2.1 Materials

$TiCl_4$(Merck, 99%), TiO_2 (Degussa P25), $AgNO_3$, Urea ($(NH_2)_2CO$), NaOHanddeionized water (DW) was used as a solvent, Chitosan [Poly (D-glucosamine)], Polyvinyl alcohol-co-ethylene, 70% propan-1-ol, 70% acetic acid.

2.2 Preparation of Doped/Undoped Tio_2 Nanoparticles

Titanium tetrachloride ($TiCl_4$) which was used as the main starting material was used as received from the supplier without any modification. A precursor of 0.1 M of 99% titanium (IV) chloride was slowly added to 200 mL of distilled water in an ice bath and stirred continuously. This was done under a fume hood because the reaction was vigorous and generating white hydrochloric gas fumes. The resultant aqueous solution was rapidly heated to 100º C to eliminate more chloride ions as hydrogen chloride.The temperature wasmaintained for 10 minutes to carry out hydrolysis and condensation to completion. The solution was then allowed to cool and neutralized to a pH of 8.0 using NaOH to aid the process of gelation. Subsequently a white gel was formed, and separated from solution by centrifugation. The precipitate was washed repeatedly with deionised water until it was free of chloride ions. This was tested by adding a few drops of $AgNO_3$solution. After a thorough wash the precipitate was filtered and allowed to dry in an oven at 150º C overnight. The dried material was then crushed and pulverized into a powder and then taken for calcination at a temperature of 600ºC at a rate of 5ºC per minute for 2 hours. Following the same proceduredescribed above, but with the addition of urea ($(NH_2)_2CO$) being added asa nitrogen source, nitrogen-doped TiO_2 was synthesized. The obtained powders were then characterized using these techniques XRD, SEM, EDX, TEM and FTIR.

2.3 Preparation of a Ag/N-TiO_2 Cs-PVAE nanofibre composite

A Cs-PVAE polymer blend of 80:20% (v/v) ratio was prepared and a measured amount of the blend was thoroughly mixed with 0.025g, 0.05g and 0.1g of TiO_2, Ag/TiO_2 and N/TiO_2nanopowders to make respective composites of the doped and undopedphotocatalysts. The nanocomposites were then taken for electrospining under a high voltage power supply that could generate up to 50 kV direct current voltages. Other apparatus used were a 25 mL syringe fitted to a capillary pipette, a metal wire and a collecting screen with aluminium foil which also acted as the grounded electrode. The metal wire was connected to the positive terminal of the power supply and passed through the capillary glass pipette. The tip of the pipette was kept 15 cm away from the grounded aluminium foil collector. The flow of the polymer blend solution was dependent on gravity and the viscosity of the solution was adjusted by changing the volume ratio of chitosan: PVAE. A voltage of 15-20 kV was applied and the polymer solution was stretched out into fibres which were then collected onto the grounded collector. Several trials were done before fibres started forming and the nanofibres were allowed to dry in air overnight and then taken for characterization by FTIR, SEM, EDX and TGA.

2.4 Characterization

TEM and SEM images were obtained for the size and morphology of nanoparticles and nanofibres respectively. The EDX spectroscopy was used for analysis of elemental components, XRD (Bruker D8 Advance) Cu $K\alpha_1$ (λ=1.5406 Å) was used for assessment of the crystalline

phases and the crystallite size of the synthesized material.A Perkin Elmer system 2000 FTIR was used to evaluate and identify the formation of functional groups formed during synthesis of the photocatalyst and nanocomposites. Using a Perkin Elmer thermogravimetric analyzer (TGA7), the thermal stability of the nanofibre was also evaluated.

3. RESULTS AND DISCUSSION

3.1 FTIR results of the TiO_2 nanoparticles

The FTIR spectrum below showsundopedtitania, N-TiO_2 and Ag-TiO_2 nanoparticles prepared by sol gel synthesis method. All three graphs show a TiO_2 characteristic broad in the region 400-900 cm^{-1} attributed to Ti-O stretching vibration and O-Ti-O lattice. The O-H bending and O-H vibrations are respectively observed in the regions 1620-1640 cm^{-1} and 3396-3500 cm^{-1} due to adsorbed water molecules and hydroxyl ions.The latter peak also corresponds to the O-H stretch region and has been attributed to the interactions between the hydroxyl groups of titania(Park *et al*., 1997; Chen *et al*., 2005; Jagadale *et al*., 2008; Suwanchawalit *et al*., 2011). Adsorbed OH ions play a central role in photocatalysis as they trap charge carriers to produce reactive OH radicals which are the driving force for the photocatalytic process. Furthermore they act as adsorbents and active sites for the reactant molecules or the pollutant (Maira *et al*., 2001). The distinct broadness of the peak in region 3379-3500 cm^{-1} in nitrogen doped titania can also be attributed to N-H symmetric and asymmetric stretching vibrations (Ren *et al*., 2007; Kong *et al*., 2010).

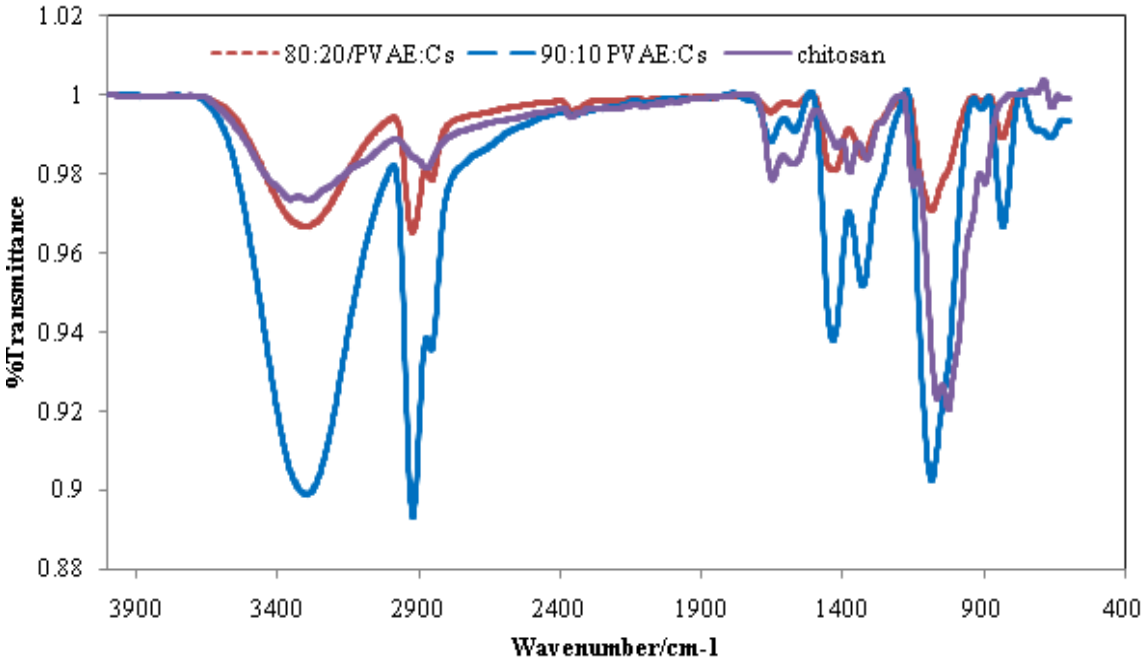

Figure 1. *FTIR spectra of doped and undoped titanium dioxide (TiO_2)*

3.2 XRD Results of the TiO_2 nanoparticles

The phase composition and crystallite sizes of the synthesized titanium dioxide nanopowders were determined by XRD analysis. The XRD patterns of the undoped as well as Ag and N doped titanium dioxide nanoparticles after calcination are shown in Figure 2 below. The samples were all calcined at 600 ºC. The XRD pattern shows that all three samples consisted of mixed crystalline phases; anatase, rutile and a small percentage of the mineral halite (NaCl) suspected to be an impurity due to the materials used in the synthesis process (Yalcin *et al*., 2010). From all the three spectra strong diffraction peaks representing the anatase phase are observed at 2θ values of 25.5º, 37.9º, 47.5º, 53.89º, 62.44º, 75.3º and 84.1º. This shows that the anatase is the dominant phase and this is beneficial since anatase is reported to be more photocatalytically active than rutile.

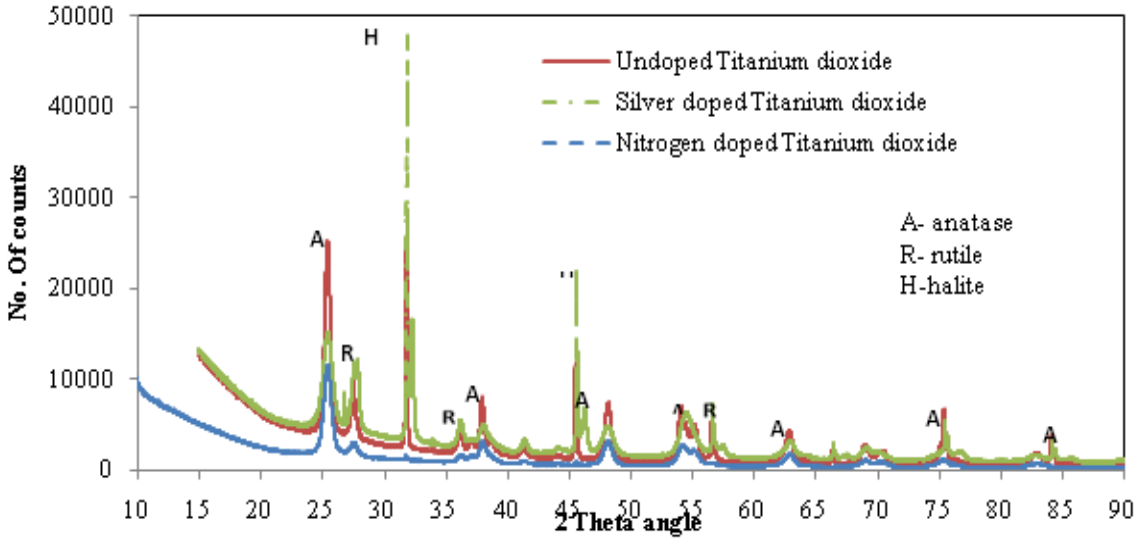

Figure 2. *XRD pattern of the doped and undopednanopowders*

Traces of the rutile phase are observed at 27.5º, 36.1º and 56.8º. From the sharpness of the peaks in the spectra it can be deduced that the calcination process induced high crystallinity(Chen *et al*., 2007; Thamaphat *et al*., 2008). On the contrary, the N-TiO_2 peak broadened after doping and the size of the crystals also decreased compared to the pure and Ag-TiO_2. This can be attributed to formation of nanoparticles and aggregation of the crystallites as they get smaller which agrees with other reported studies (Sathish *et al*., 2005; Chen *et al*., 2005). The Scherrer equation has been used to estimate the average sizes of the nitrogen doped titania nanoparticles where it was deduced that a decrease in peak width is directly proportional to the size of nanoparticles.

Silver doped TiO_2 spectrum does not show any noticeable change in the number of peaks due to the presence of the silver dopant. Nasr-Esfahani *et al*., (2008) suggests that this could imply that the Ag nanoparticles were well scattered on the surface of TiO_2. Behnajady *et al*., (2008) points out that this could be due to what has been reported by other researchers that silver attaches on the surface of titania since it has a large radius to be incorporated into the lattice structure (Sobana *et al*., 2006; Choi *et al*., 2009).

The Scherrer equation was used to estimate the average size of titanianocrystallite. Nitrogen doped titania had an average grain size of 8.2 nm, and this was the smallest size compared to undopedtitania and Ag doped TiO_2 with 9.23 nm and 10.52 nm respectively. These estimated results confirm what has been reported that peak broadening in nitrogen doped TiO_2 implies formation and agglomeration of nanoparticles (Sathish *et al*., 2005; Kusumawardani *et al*., 2009). The size of nanoparticles and the surface are said to have an inversely proportional relationship, implying that N-doped TiO_2 has a larger surface area compared to the undoped and Ag-doped nanoparticles (Sobana *et al*., 2006).

3.3 SEM and EDX results

To examine the morphology of the synthesized nanoparticles and electrospun nanofibres, SEM analysis was carried out on the JEOL JSM-6390LV SEM fitted with secondary electron detector, and equipped with an attachment for the Energy dispersive X-ray spectroscopy (EDX) to enable elemental composition analysis. The SEM micrograph of these nanomaterials is shown in Figure 3 below. From Figure 3a spherical shaped TiO_2 nanoparticles show an even distribution and Figure3b shows the electrospun nanofibres made from a polymer blend of chitosan/ PVAE and titania nanoparticles. The average size of the nanofibres was found to be in the range 234-270 nm, and appeared to be uniform.

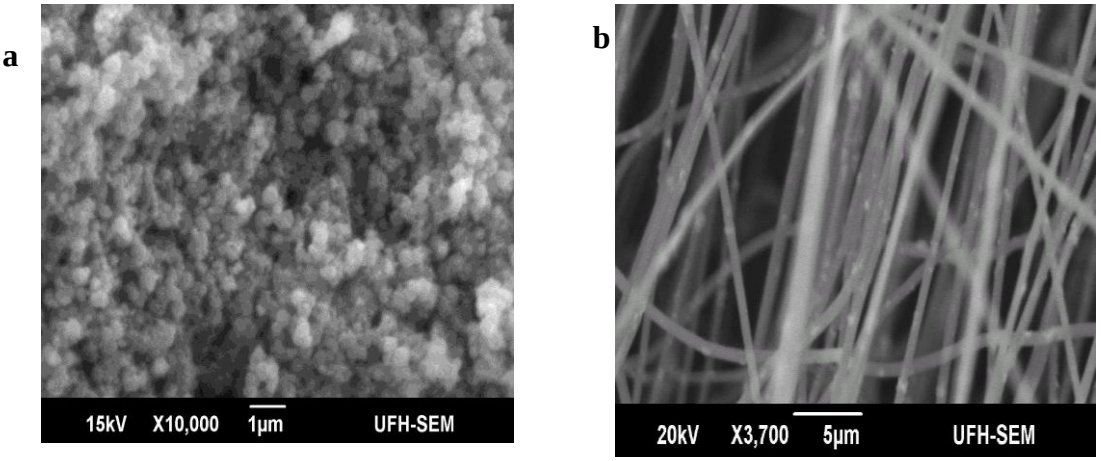

(a) SEM image of undoped TiO_2 spherical icles

(b) SEM image of TiO_2-Cs/PVAE nanofibres

Figure 3. *SEM images (a) undoped TiO_2 spherical nanoparticles (b) TiO_2 nanoparticles immobilized on Cs-PVAE polymer blend*

EDX analysis for elemental composition ofundopedtitania, nitrogen and silver doped titania was done. The high weight % oftitanium and oxygen showsthat they are the main components. The weight % loading of the dopant in Ag-TiO_2(11.99%) was much higher compared to that of N-TiO_2(3.18%) and this can be suggested to be due to silver dopant attaching onto the surface of titania and not incorporated into the crystal lattice in which case it would be shadowed from detection. Nitrogen has a small radius which is comparable to that of oxygen; therefore it can easily undergo interstitial substitution into titania(Choi *et al*., 2009; Sobana *et al*., 2006). Hence, only a small fraction of nitrogen weight % was detected compared to the silver weight %.

3.4 TEM results

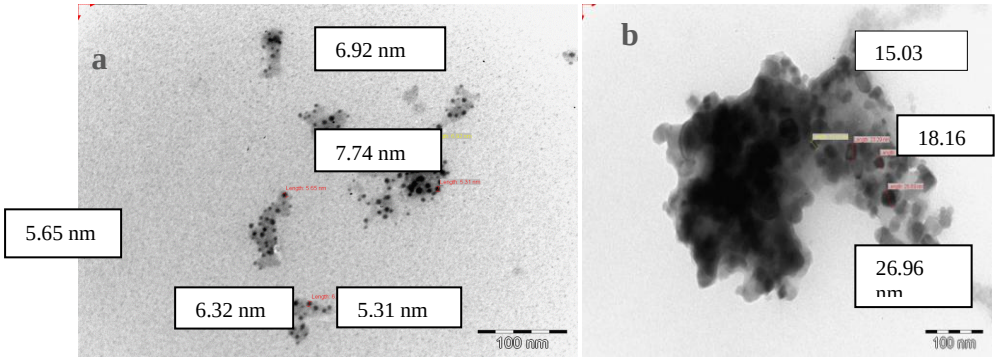

(a) TEM image N doped TiO_2 nanoparticles

(b) TEM image of Ag doped TiO_2 nanoparticles

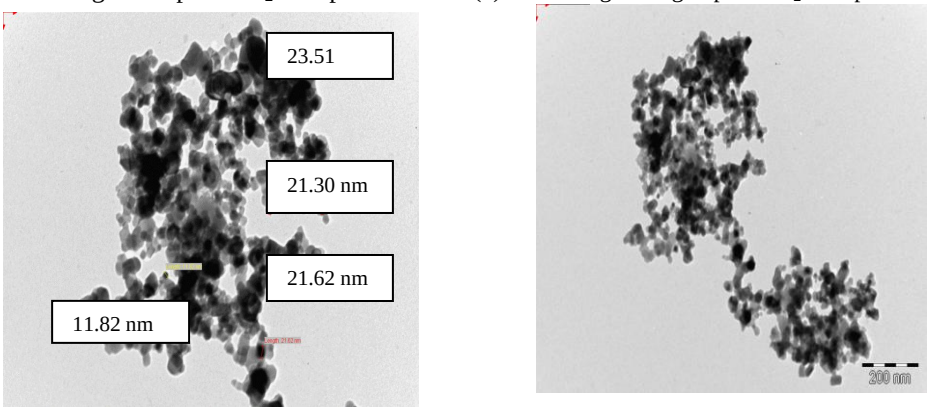

(c)TEM image of undoped TiO_2 nanoparticles (zoomed)

Figure 4. *TEM images of doped and undoped TiO2 nanoparticles*

Nanoparticle size measurement was obtained through TEM analysis. Figure 4 below depicts TEM images of doped and undoped TiO_2 nanoparticles (images a-d) after calcination. The micrographs show that nanoparticles are spherical in shape confirming the images of the SEM.The average size determined from the diameter of randomly selected nanoparticles ranged from 6.4 nm to 21 nm and this is comparable to the estimated nanoparticles sizes as calculated from the XRD results. Figure 4(a) shows N-doped TiO_2 nanoparticles which appear to have a crystalline monodisperse orientation compared to Ag-doped TiO_2 in Figure 4(b) and the undopedtitania in images (c) and (d) which appear to be aggregated and polydisperse. The size of the undopedtitania in Figures 4 (c & d) is comparable to the reported size of commercial P25 TiO_2 which ranges between 21-30 nm (Bakardjieva *et al*., 2005).

3.5 FTIR Results of the Electrospun Nanofibres

FTIR analysis spectra for the electrospun nanofibres were obtained to identify the structural changes that took place during the process. Figure 5 depicts the FTIR spectra of pure chitosan (curve A), the 90:10% (v/v) (curve B) and 80:20 % (v/v) (curve C) blends of PVAE and chitosan. Spectrum A shows peaks that are characteristic of chitosan, a sharp peak observed in the wavenumber range from 1018 cm^{-1} correspond to the C-O stretching vibration and peaks in the range 842-1120.6 cm^{-1} are assigned to the saccharide structure of chitosan. Peaks at 1332 cm^{-1} and 1363 cm^{-1} are characteristic of the CH_3 symmetric deformation and stretching vibration of C-H bonds. Another C-H stretching vibration was observed at the peak 2889 cm^{-1}. These peaks can also be attributed to symmetric or asymmetric CH_2 stretching from the pyranose ring. The peaks at 1577 cm^{-1} and 1654 cm^{-1} respectively correspond to the stretching vibration of the amino and amide group of chitosan. The broad but not intense peak in the range 3200-3400 cm^{-1} is due to the amine NH symmetric vibration (Pawlak *et al*., 2003; Krishna Rao *et al*., 2006; Anicuta *et al*., 2010).

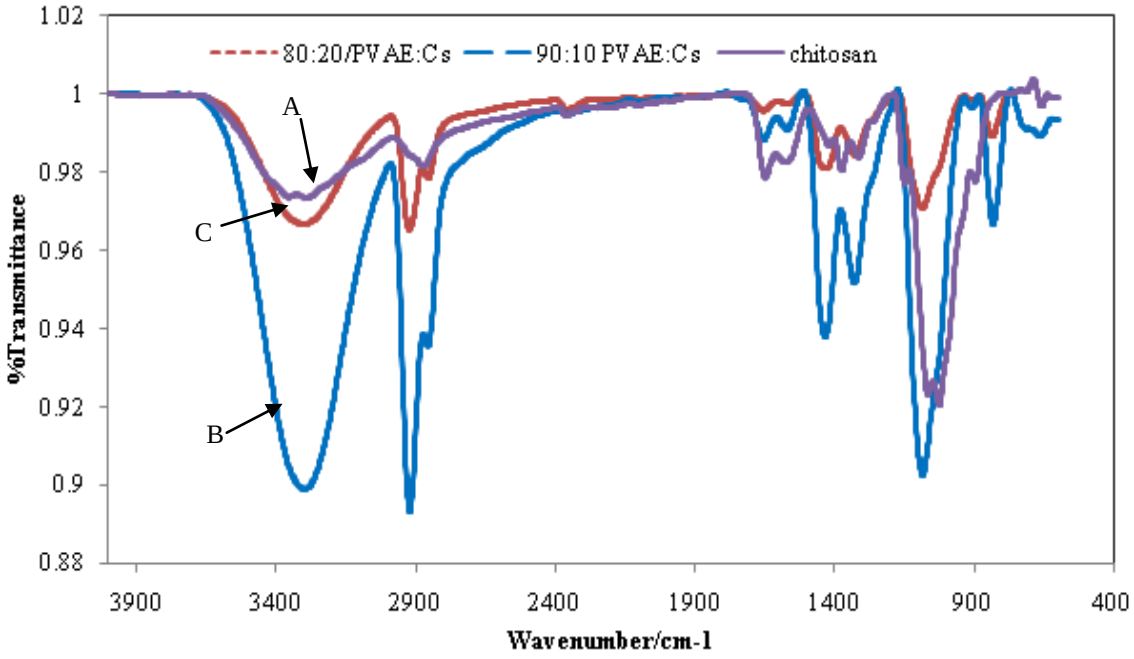

Figure 5. *FTIR of pure chitosan and chitosan blended with PVAE*

Spectrum B where the ratio of PVAE to chitosan is 90:10 % (v/v) depicts peaks that are typical of PVAE. A broad peak in the range 3200-3400 cm^{-1} represents –OH and –NH stretching vibrations of the hydroxyl group in PVAE and amine group in chitosan. The intensity of the peaks in spectrum B is decreased when chitosan content is increased to make the volume ratio of the polymers 80:20 % (v/v). These observations suggest that hydrogen bonding between the two polymers occured even though most of the chitosan peaks overlapped with PVAE peaks (Krishna-Rao *et al*., 2006; Jia *et al*., 2007). The disappearance of the -NH peak in spectra B and C can be attributed to the fact that the amount of chitosan in the blend is low compared to that of PVAE suggesting that chitosan peaks are masked.

3.6 TGA results

TGA analysis was employed to determine the thermal stability and degradation temperature of the synthesized nanoparticles and electrospun nanofibres. Figures 6, 7 and 8 show the normal thermograms (TGA) and the differential thermograms (DTG) of PVAE: Cs polymer blends with different volume ratio. These thermograms show the degradation of the polymers as the temperature increases. All the thermograms show a multiple stage degradation with two visible weight losses or degradation stages observed around 100-120 ºC and the other in the range of 400-550 ºC. The first weight loss around 100º C corresponds to the loss of moisture and water adsorbed onto the nanofibres (Pawlak *et al*., 2003). The major weight loss observed in the range 400-460 ºC is due to the degradation of the polymer blend, mainly PVAE which is reported to degrade in one step starting from a temperature of 380 ºC (Dutra *et al*., 1996). PVAE is mainly composed of polyvinyl alcohol (PVA) which is known to undergo thermal degradation around 400 ºC, therefore the weight loss at 407.7 ºC corresponds to the breaking down of the PVA moiety in the blend (Juntanon *et al*., 2008).

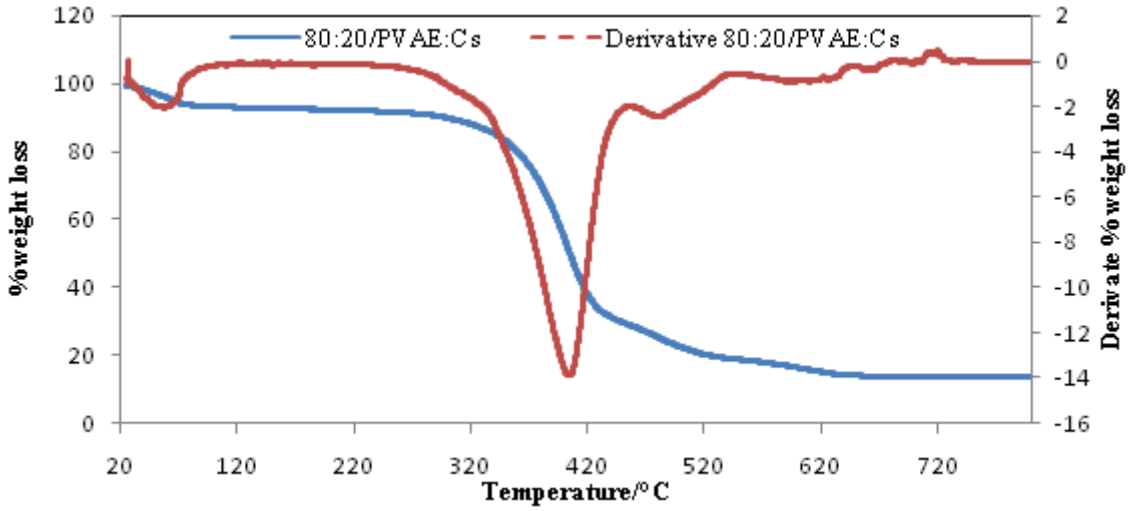

Figure 6. *Thermogram and differential thermogram of 90:10% (v/v) PVAE:Cs polymer blend*

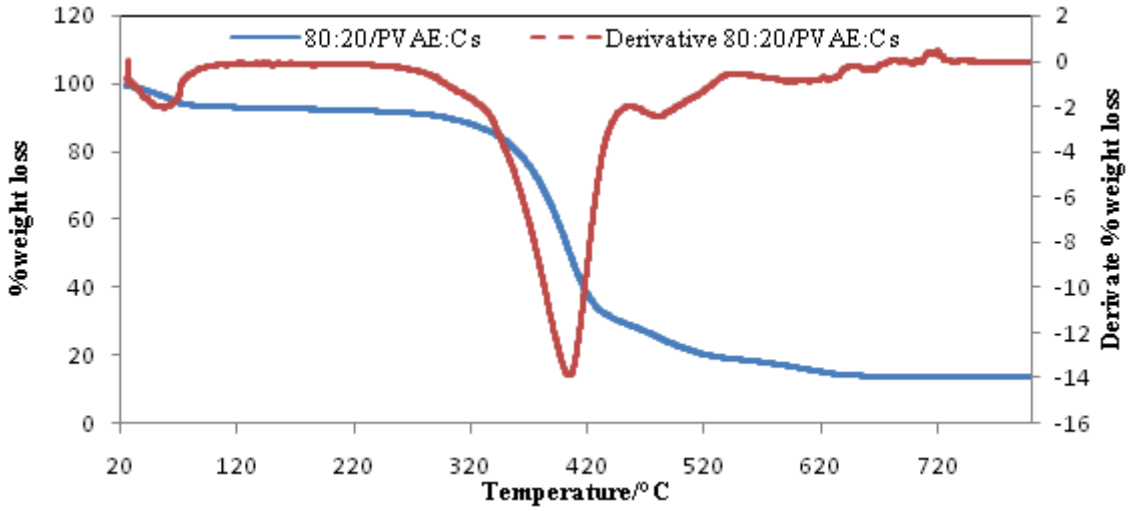

Figure 7. *Thermogram and differential thermogram of 80:20% PVAE:Cs polymer blend*

It is however observed in the DTG thermograms of the polymer blends in Figure 8 that as the amount of chitosan was increased from 90:10% PVAE:Cs to 80:20% (v/v) a shift in the peaks occurred. The degradation temperature of the polymer blend (PVAE-Cs) decreased to a lower temperature (458 ºC to 407.7 ºC). This shift is owed to the increase in volume of chitosan because it corresponds to the thermal degradation and deacetylation of chitosan (Qu*et al*., 2000). Furthermore this change confirms the interaction between chitosan and PVAE.

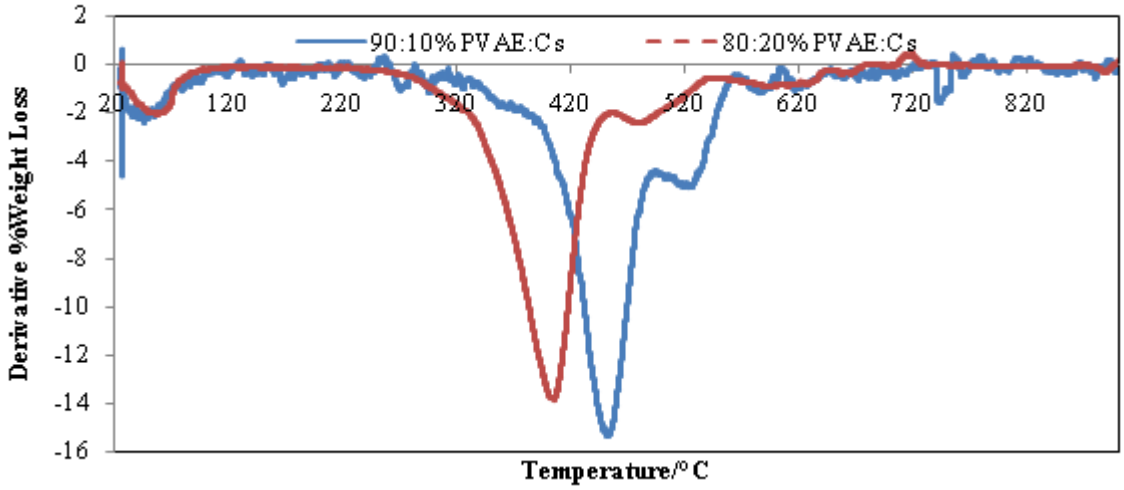

Figure 8. *Differential thermograms of 90:10% and 80:20% (v/v) of PVAE:Cs polymer blends*

4. Results and Discussion of Application Tests

Conclusions and Recommendations

The sol gel synthesis method is advantageous because many parameters such as temperature, pH and concentration of dopants can be controlled during the process. Moreover sol-gel is suitable for doping reactions since it helps to develop strong interactions between the dopant and photocatalyst or support (Lopez Goeme *et al*., 2012). Nitrogen and silver doped titanium dioxide nanoparticles were successfully synthesized and this was confirmed through various characterization techniques; FTIR, TEM, SEM, and EDS. From the XRD results it was deduced that the selected calcination temperature of 600 ºC for 2 hours was best suited for production of highly crystalline nanomaterials.

Using the electrospinning method, the prepared nanopowders of Ag and N doped TiO_2 were immobilized onto the nanofibres of a polymer blend of chitosan and polyvinyl alcohol-co-ethylene. The electrospun nanofibres were characterized by SEM to determine fibre orientation and size. The SEM images showed that the fibre had a uniform distribution and looked like mats.

References

[1] Arnel, N. (2004). Climate change and global water resources: SRES emission and socio-economic resources. Global Environmental Change, 14, 31-52.

[2] Savage, N., Diallo, M., Duncan, J., Street, A., Sustich, R. (2009). NanotechnologyApplications for Clean Water. Norwich, NY: William Andrew Inc.

[3] Shannon, M.A., Bohn, P.W., Elimelech, M., Georgiadis, J.G., Marinas, B., Mayes, A.N. (2008). Science and technology for water purification in the coming decades. Nature, 452, 301-310.

[4] Choi, H., Stathatos, E., Dionysiou, D.D. (2007). Photocatalytic TiO2 films and membranes for the development of efficient wastewater treatment and reuse systems. Desalination, 202 (1-3), 199-206.

[5] Nor, H., Iis, S. . (2009). Nanosized TiO2 photocatalyst powder via sol-gel method: Effect of hydrolysis degree on powder properties. International Journal of Photoenergy, 2009, 1-8.

[6] Nosaka, Y., Matsushita, M., Nishino, J., Nosaka, A.Y. (2005). Nitrogen-doped titanium dioxide photocatalysts for visible response prepared by using organic compounds. Science and Technology of Advanced Materials, 6 (2), 143-148.

[7] Kim, D.H., Choi, D., Kim, S., Lee, K.S. . (2008). The effect of phase type on photocatalytic activity in transition metal metal doped TiO2 nanoparticles. Catalysis Communications, 9, 5, 654-657.

[8] Su, B., Liu, X., Peng, X., Xiao, T., Su, Z. (2003). Preparation and characterization of the TiO2/polymer complex nanomaterial. Materials Science and Engineering, A349, 59-62.

[9] Jagadale, T.C., Takale, S.P., Sonawane, R.S., Joshi, H.M., Patil, S.I., Kale, B.B., Ogale, S.B. (2008). N-doped TiO2 nanoparticle based visible light photocatalyst by modified peroxide sol-gel method. Journal Phys. Chem., 14596-14602.

[10] Suwanchawalit, C., Chanhom, P., Sriprang, P., Wongnawa, S. (2011). Ag-Doped TiO2 photocatalyst for dye decolorization under UV. Pure and Applied Chemistry International conference, pp.375-405.

[11] Maira, A.J., Coronado, J.M., Augugilaro, V., Yeung, K.L., Conesa, J.C., Sorla, J. (2001). Fourier Transform Infrared Study of the Performance of Nanostructured TiO2 particles for the photocatalytic oxidation of gaseous toluene. Journal of Catalysis, 202, 413-420.

[12] Ren, L., Huang, X., Sun, F., He, X. (2007). Preparation and characterization of doped TiO2 nanodandelion. Materials letters, 61, 2, 427-431.

[13] Kong, H., Song, J., Jang, J. . (2010). Photocatalytic Antibacterial Capabilities of TiO2-Biocidal Polymer Nanocomposites Synthesized by a Surface-Initiated Photopolymerization. Environmental Science and Technology, 44, 5672-5676.

[14] Yalcin, Y., Kilic, M., Cinar, Z. (2010). The role of non-metal doping in TiO2 photocatalysis. J. Adv. Oxid. Technol. , 13, 3, 281-296.

[15] Chen, X., Mao, S.S. (2007). Titanium Dioxide Nanomaterials: Synthesis, Properties, Modifications, and Applications. Chemical Reviews , 107, 7, 2891-2959.

[16] Thamaphat, K., Limsuwan, P., Ngotawornchai, B. (2008). Phase characterization of TiO2 powder by XRD and TEM. Kasetsart J. (Nat. Sci.), 42, 357-361.

[17] Sathish, M., Viswanathan, B., Viswanath, R.P., Gopinath, C.S. (2005). Synthesis, Characterization, Electrosnic Structure, and Photocatalytic Activity of Nitrogen-Doped TiO2 Nnaocatalyst. . Chemical Materials, 17, 25, 6349-6353.

[18] Chen, X. L. (2005). Formation of Oxynitride as the Photocataltic Enhancing Site in Nitrogen-Doped Titania Nanocatalysts: Comparison to a Commercial Nanopowder. Advanced Functional Materials, 15, 1, 41-49.

[19] Nasr-Esfahani, M., Habibi, M.H. (2008). Silver Doped TiO2 Nanostructure Composite Photocatalyst Film Synthesized by Sol-Gel Spin and Dip Coating Technique on Glass. International Journal of Photoenergy, 628713, 1-11.

[20] Behnajady, M. M. (2008). Enhancement of photocatalytic activity of TiO2 nanoparticles by Silver doping: Photodeposition versus Liquid impregnation methods. Global NEST Journal, 10, 1, 1-7.

[21] Sobana, N., Muruganadham, M., Swaminathan, M. (2006). Nano-Ag particles doped TiO2 for efficient photodegradation of direct azo dyes. Journal of Molecular Catalysis A: Chemical , 258, 124-132.

[22] Choi, J., Park, H., Hoffmann, M.R. . (2009). Effects of Single metal-ion doping on the visible light photo-reactivity of TiO2. Journal of Physical Chemistry, C, 17-55.

[23] Kusumawardani, C., Kartini, I., Narsito,. (2009). Synthesis of visible light active N-doped Titania photocatalyst . International Conference on Chemical, Biological and Environmental Engineering (pp. 115-118). Singapore: World Scientific Publishing Co. Pte.

[24] Bakardjieva, S., Subrt, J., Stengl, V., Dianez, M.J. (2005). Photoactivity of anatase-rutile TiO2 nanocrystalline mixtures obtained by heat treatment of homogeneously precipitated anatase. Applied Catalysis, 58, 193-202.

[25] Pawlak, A., Mucha, M. (2003). Thermogravimetric and FTIR studies of chitosan blends. Tehmochimica Acta, 396, 153-166.

[26] Krishna Rao, K.S.V., Vijaya Kumar Naidu, B., Subha, M.C.S., Sairam, M., Aminabhavi, T.M. (2006). Novel chitosan-based pH-sensitive interpenetrating network hydrogels for the controlled release of cefadroxil. Carbohydrate Polymers, 66, 333-344.

[27] Anicuta, S. D. (2010). Fourier transform infrared (FTIR) spectroscopy for characterization of antimicrobial films containing chitosan . Analele Universitatii din Oradea Fascicula: Ecotoxicologie, Zootehnie si Tehnologii de Undustrie Alimentara, 1234-1240.

[28] Jia, Y.T., Gong, J., Gu, X.H., Kim, H.Y., Dong, J., Shen, X.Y., . (2007). Fabrication and characterization of poly (vinyl alcohol)/chitosan blend nanofibres produced by electrospinning method. Carbohydrate Polymers, 67, 403-409.

[29] Dutra, R. L. (1996) Poly (ethylene-co-vinyl alcohol-co-vinyl mercaptoacetate) (EVALSH)-determination of the vinyl mercaptoacetate content by thermogravimetric analysis and FTIR spectroscopy. Polymer Bulletin, 36, 593-600.

[30] Juntanon, K., Niamlang, S., Rujiravanit, R., Sirivat, A. (2008). (2008). electrically controlled release of sulfosalicylic acid from crosslinked poly (vinyl alcohol) hydrogel. International Journal of Pharmaceutics, 356, 1-2, 1-11.

[31] Qu, X., Wirsen, A., Albertsson, A.-C. (2000). Effect of lactic/glycolic acide side chains on the thermal degradation kinetics of chitosan derivatives. Polymer, 41, 4841-4847.

[32] Lopez Goeme, T.M., Alvarez Lemus, M.A., Angeles Morales, V., Gomez Lopez E., Castillo Ocampo, P. (2012). Study of Bacterial Sensitivity to Ag-TiO2 Nanoparticles. J. Nanomedicine & Nanotechnology, S5, 1-7.

[33] Park, H.K., Kim, D.K., Kim, C.H. (1997). Effect of Solvent on Titania Particle Formation and Morphology in Thermal Hydrolysis of TiCl4. Journal American Ceramic Soc. , 80, 3, 743-749.

.